

# Motion Tracking Smart Work Suit With a Modular Joint Angle Sensor Using Screw Routing

Jewoo Lee , Kyu-Jin Cho , and Useok Jeong , *Member, IEEE*

**Abstract**—Activity data of workers can be used to manage their safety and working processes. To date, the adoption of motion measuring systems in industrial sites has been limited, due to cost and noisy environments. In this study, a motion-tracking smart work suit is presented to monitor the movements of workers. This system comprises modular joint-angle sensors that utilize a BoASensor mechanism, a conventional work suit with added sensor sleeves, and a monitoring device. The modularized joint-angle sensor can be easily attached or detached onto or from the normal work suit, improving its usability and washability. This suit could experience relative motion and deformation between the body, degrading sensor robustness, unlike conventional motion sensing suits. The screw sensor routing method is proposed to minimize the coordination effect between the sensor and skeletal system during body movements. Various postures recorded with the suit exhibited root mean square errors lower than 7.75% from the elbow range of motion (150°) compared with the inertial-measurement-unit-(IMU)-based motion tracker. It was determined that there exists statistical significance between the proposed screw-routing method and the IMU in precision, thereby demonstrating sensing robustness with various upper limb motions. Additionally, the linearity analysis revealed that screw-routing has the highest linear behavior. The proposed work suit is expected to be utilized in preventing industrial accidents at various sites, owing to its low production cost and high accessibility.

**Index Terms**—BoASensor, motion sensing, sensor routing, smart work suit.

## I. INTRODUCTION

The manufacturing process has been considered a human-in-the-loop system that involves both the manufacturing equipment and operator [1]. To optimize the overall manufacturing output, the process parameters of the manufacturing device and the status of the operator should be monitored [2]. If the

Manuscript received 24 February 2022; accepted 1 July 2022. Date of publication 25 July 2022; date of current version 4 August 2022. This letter was recommended for publication by Associate Editor K. Kyung and Editor C. Laschi upon evaluation of the reviewers' comments. This work was supported in part by the National Research Foundation of Korea (NRF) funded by the Korea Government, MSIT, under Grant 2019R1F1A1041277 and in part by the Korea Institute of Industrial Technology through the Development of Soft Robotics Technology for Human-Robot Coexistence Care Robots under Grant KITECH EH220002. (Corresponding author: Useok Jeong.)

Jewoo Lee and Kyu-Jin Cho are with the Biorobotics Laboratory, Department of Mechanical and Aerospace Engineering, Institute of Advanced Machines and Design, Soft Robotic Research Center, Seoul National University, Seoul 08826, Republic of Korea (e-mail: jwlee2218@snu.ac.kr; kjcho@snu.ac.kr).

Useok Jeong is with the Robotics R&D Department, Korea Institute of Industrial Technology (KITECH), University of Science & Technology (UST), and HYU-KITECH, Ansan-si 15588, Republic of Korea (e-mail: snopyy86@gmail.com).

Digital Object Identifier 10.1109/LRA.2022.3193450

measurement of worker variables, such as individual work hours, amount, speed, and pattern is accessible, the data could be used to monitor workers' health, as well as manage workloads [3]. Moreover, with individual work patterns and workload management, it would be possible to prevent industrial accidents [4], [5].

Conventional body movement measuring sensors, including optical [6] and inertial measurement unit (IMU) sensors [7], are not suitable for application in the manufacturing environment [23], [8], despite the fact that they can accurately record motions, there is a blind spot for cameras and IMUs are not currently affordable enough for daily tracking. The goniometers such as optical-fiber based device [9], are not cost efficient to utilize in work environments or daily life. If directly embedding the motion sensor onto the existing work suit without interfering with the movement is possible, the operator status can be monitored without affecting the work performance or environment. Moreover, to be utilized in a manufacturing environment with several workers, the sensor should be manufactured at a low unit price.

An alternative approach to avoid disturbances on the wearer during the measurement, is using deep learning-based vision analyses. Commercialized motion tracking devices for home entertainment – Kinect [10], [11] and Nintendo Wii [12] – are not needed to attach additional markers or wearable sensors. Instead, they use cameras and separate controllers, making it difficult to apply these devices to work environments. Attempts have been made to monitor workers' postures using depth images [13]; however, they have limitations when applied to real industrial sites owing to the dynamic environment.

Another approach is to use soft stretch sensors. Soft stretch sensors have been developed based on soft polymers with capacitive or resistive sensing mechanisms to measure the angle of the fingers [14], [15], or knee and elbow [16], [17]. However, polymer type sensors are prone to be challenged with fabrication failure and hard to be mass produced [18]. Commercial stretch sensors which utilize resistance-varying characteristics of rubber under expansion/contraction are offered with affordable costs and easy fabrication [19], but show high hysteresis and small measurement range. Moreover, posture-dependent wrinkles and relative movement between the cloth and the body degrade measuring robustness in wearable type soft sensors. Yuen et al. [20] proposed a sleeve-type angle-measuring device that can calibrate errors due to wrinkles. However, strain gauges that are utilized to measure the angles should be strictly attached to the limbs, and are not suitable for daily usage [21].

In this study, a motion tracking smart work suit in which the sensor can be easily attached and detached from the existing work suit with a simple modification by adding a sensor pouch is introduced. Several methods have been compared to minimize



Fig. 1. Schematic of proposed motion-sensing smart work suit system comprising a traditional working suit, wireless bend sensing module, charging station, and monitoring devices.

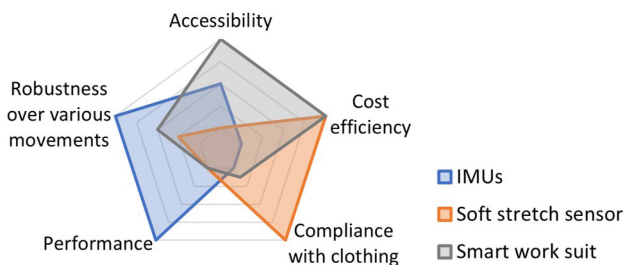


Fig. 2. A comparison of the characteristics of the IMUs, the soft stretch sensor, and the smart work suit.

the effect of sensor dislocation relative to the body joint originating from the body postures and posture-dependent wrinkles of the cloth. The screw sensor routing method is selected to maximize the sensing robustness of the smart work suit. The suit is designed to measure the joint movements of workers without interrupting postures and work efficiency. Moreover, it offers a great possibility of mass production at a low cost, enabling application to groups of workers.

## II. SMART WORK SUIT

The motion measurement smart work clothes system (Fig. 1) developed in this study mainly comprises 1) a bend sensor and charging station, 2) a work suit with jacket and trousers, and 3) software for wireless data acquisition. By sewing a polyester sleeve to route the bend sensor to the existing work suit, it is possible to easily transform off-the-rack clothes into smart work clothes. The BoASensor mechanism [22] is adopted for the bend sensor module, which is thin, robust, and inexpensive for use in a work suit.

### A. Characteristics

Fig. 2 illustrates the characteristic comparison of motion sensing system with IMUs, soft stretch sensors, and smart work suit. In terms of the IMU system, it has the highest performance and is able to distinguish the angle of a target joint from various movements with multi-degrees-of-freedom sensing capability. However, it is currently not affordable and requires a calibration process with a biomechanical model. Soft stretch sensors are cost-effective and compatible with clothing. However, there are currently few soft sensors available on the market and they

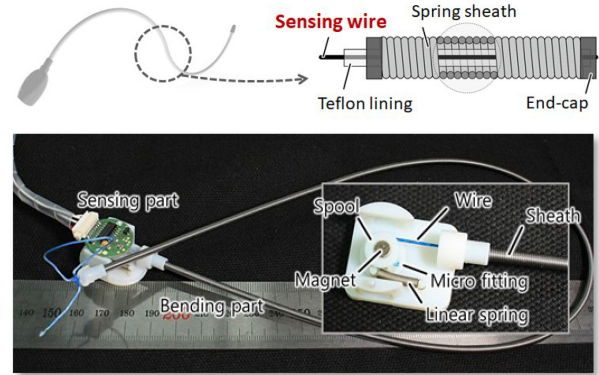


Fig. 3. Basic structure of BoASensor mechanism measuring bending angle along the spring sheath. It comprises a sensing wire, Teflon lining, spring sheath, and encoder.

require special materials for fabrication. The Smart Work Suit System fills the gap between these two systems since it can be fabricated using off-the-shelf components and directly measures joint angles providing accessibility. Additionally, the proposed screw routing method is robust enough to measure the target joint in a variety of postures and motions.

### B. Joint Angle Measurement

Fig. 3 illustrates the basic structure of BoASensor [22] for measuring the joint angle. The proposed sensing mechanism measures the bend angle along the coil sheath by using the translational position of the sensing wire as the sheath is bent. The rotational angle of the spool, which is wound by the sensing wire, can be measured using a Hall-effect sensor, and the measured value can be converted to the bend angle of the spring sheath. The advantages of the BoASensor on the motion sensing work suit are the thin foam factor, enabling easy insertion into the suit, and a simple mechanism enabling robust and low-cost design.

For the bending part of the sensor, a polytetrafluoroethylene (PTFE)-coated coil is utilized in this study to protect it from external contamination, making the sensor insertion easier and reducing puckering with a low friction coefficient. In addition, the coil diameter is reduced to  $\phi 2.0$  mm to minimize movement disturbance and give the visual impression that the sensor is not attached. The minimum spool size is selected for the sensor by considering the movement range of the human body joints (less than  $180^\circ$ ) and displacement of the inner tendon according to the coil diameter. The neodymium magnet ( $\phi 3.0$  mm) for measuring the angle of the spool acts as a tendon spool, minimizing the number of parts and assembly process.

The developed bending sensor to measure the joint angle is easily charged through the charging station, as illustrated in Fig. 4, and its compact size ( $25 \text{ mm} \times 25 \text{ mm} \times 10 \text{ mm}$ ;  $\phi 2 \times 150 \text{ mm}$ ; Fig. 5) does not interfere with the movements of the wearer or impair the aesthetics even when attached to clothes.

### C. Electronics

To wirelessly transmit the acquired data, the iBeacon protocol based on the Bluetooth Low Energy (BLE) method is selected. iBeacon enables 1:n data transmissions without an additional pairing process, improving the degree of freedom for the IoT function. In the developed device, the sensor module ID and

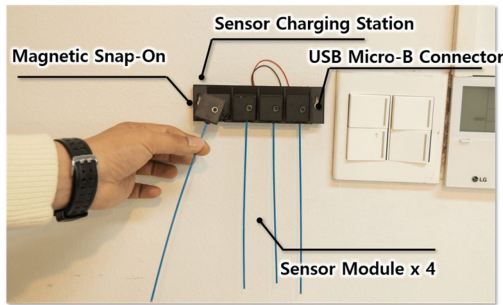


Fig. 4. Charging station for ease use of the motion-sensing system. One set of the sensing module comprises four sensing modules for the left and right sides of the elbow and knee, respectively.

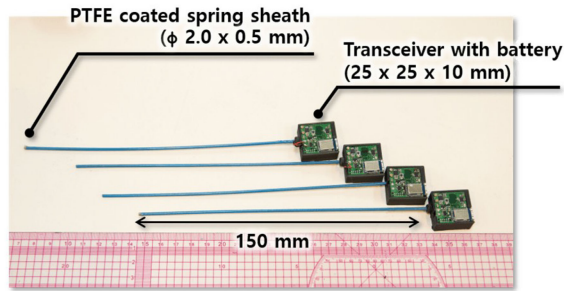


Fig. 5. Wireless bend sensing modules with embedded batteries. The bend sensing part comprises a thin PTFE coated spring sheath with diameter =  $\Phi 2.0$  and length = 150 mm. The electronic part comprising a transceiver and a battery ( $25 \times 25 \times 10 \text{ mm}^3$ ) is connected to the spring sheath.

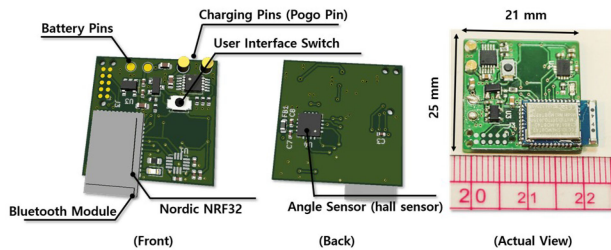


Fig. 6. Electronic module for bending angle measurement and wireless broadcasting. It consists of a hall-effect sensor with ADC for the measurement of translation of the sensing wire, NRF32 (Nordic Semiconductor) processor with embedded Bluetooth interface, and a Li-Po battery (3.5 V, 58 mAh) for 10-h operation.

angle measurement values are broadcast so that the monitoring device can integrate the values of all available sensors. Other electronic components were designed to minimize the board size and increase the usability (Fig. 6). A soft switch is utilized to control the board mode. Currently, it can turn the board into sleep mode and can be further utilized for user interfaces. The board is charged by connecting the Pogo spring-loaded pins on the board with the magnetic switch. NRF32 from Nordic Semiconductor is used for signal filtering and BLE interface. The electronics is equipped with Li-Po battery (3.5 V, 58 mAh) for 10-h operation covering daily working hours.

#### D. Work Suit Design – Sensor Placement

1) *Sensor Routing Methods*: Fig. 7 illustrates the possible candidates required for the sensor routing used for joint angle

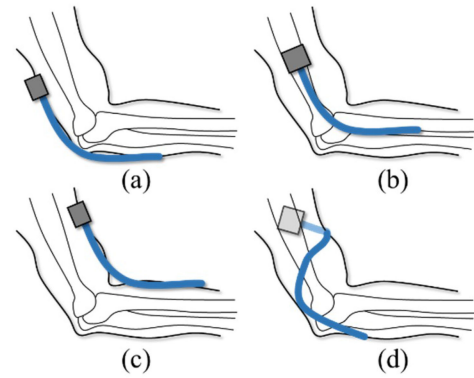


Fig. 7. Possible attachment points of the bend sensor for measuring joint angle: (a) dorsal, (b) lateral, (c) anterior, and (d) screw routing.

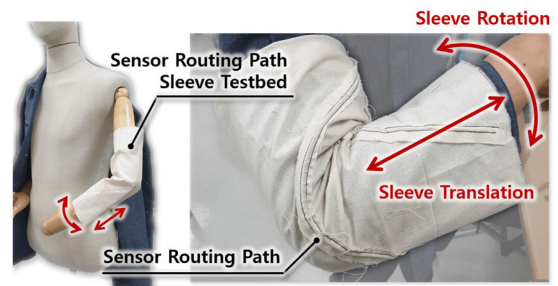


Fig. 8. Testbed for investigating the posture-dependent sensor dislocation for each sensor routing methods (left), relative translation and rotation of the sleeve between the body with a screw routing example (right).

sensing: (a) dorsal, (b) lateral, (c) anterior, and (d) screw routing. The physical characteristics of the sensor should be considered when choosing the best place to attach the sensor to the joint. The soft stretch sensor has to be attached passing through the dorsal part of the joint orthogonal to the joint axis, as illustrated in Fig. 7(a), to generate stretching when the joint bends [14]–[17]. Moreover, stretch-type sensors should be attached directly onto the skin or spandex tights to allow the sensor to properly stretch without slipping. Bend-type sensors can be attached to the lateral side of the joints (Fig. 7(b)) [23], similar to the conventional goniometer [24] to place the transducer on the rotational axis of the joint.

The BoASensor, however, can be placed in several directions (Fig. 7) as the sensor has a wide sensing area and can be inserted into the sleeve of the cloth because of its thin form factor and axial stiffness. The working suit, unlike spandex tights is vulnerable to measurement errors during the wearer's movements because of the relative motion between the body and cloth [25], [26], for example, rotation and translation of the suit's sleeve as depicted in Fig. 8. Furthermore, pose-dependent wrinkle [27]–[29] and sensor routing path-dependent buckling can be generated on the sleeves, which cause sensor routing deviation relative to the target joint. These factors significantly influence the sensing accuracy, robustness, and wear comfort. This study proposes a screw sensor routing method that enhances sensing robustness against pose-dependent wrinkles in a working suit. Three routing methods are compared—dorsal, lateral, and screw—based on wearer comfort, measuring accuracy, and robustness.



Fig. 9. Three sensor routing methods—(a) dorsal, (b) lateral, (c) screw—for the elbow flexion/extension and two routing methods—(d) dorsal and lateral—for knee flexion/extension. (a) Rotation of the sleeve regarding the body cause measurement error due to sensor misalignment. (b) Lateral routing of the bend sensor makes wrinkling and buckling of the cloth degrading sensing robustness as well as wear comfort. (c) Screw sensor routing for the measurement of elbow provides tight sensor fit along the joint, minimizing posture-dependent sensing error of the smart work suit.

Fig. 9 illustrates prototypes of three sensor routing methods for elbow—(a) dorsal, (b) lateral, (c) screw—and two routing methods for knee—(d) dorsal and lateral. The anterior routing method in Fig. 7(c) is excluded in this study because it significantly decreases wear comfort and is sensitive to buckling. The sleeves of the work jacket are prone to rotate and translate along the arm because they have a loose fit, unlike the spandex tights for the motion capturing system. Fig. 9(a) illustrates the shoulder posture that generates sleeve rotation. It transforms dorsal routing to lateral routing, which results in sensing data variation as the bend angle of the sensor does not remain consistent during

sleeve rotation. Fig. 9(b) illustrates the fabric deformation on the lateral side of the sleeve during elbow flexion [29], which is also called a half-lock fold. This wrinkle is generated when the compressive force is applied to the anterior side of the sleeve, and the crease line propagates to the lateral side. The insertion of the bend sensor along the lateral line blocks the propagation of the crease line, thereby limiting the cloth's strain, causing discomfort to the user [30], and generating posture-dependent sensing errors. Fig. 9(d) illustrates the dorsal and lateral sensor routing on the knee, which is similar to elbow routing. Trousers do not exhibit posture-dependent sleeve rotation, illustrated in Fig. 9(a), owing to the limited range of motion of the hip. However, wrinkles owing to half-lock folds have been observed to affect the lateral sensor routing of the knee.

Fig. 9(c) illustrates the screw routing of the bend sensor around the elbow joint, which is proposed in this study. The screw routing places the bend sensor diagonal to the axial direction of the elbow and rotationally wraps the elbow joint. The concept of screw routing involves avoiding the fold or crease line of the fabric due to sensor insertion during various postures of the upper limbs by routing the bending sensor to follow the points of tension on the sleeve. It has been observed that screw sensor routing does not generate wrinkles, buckling, or crease lines in various upper limb postures, which is experimented in the following chapter. As illustrated in Fig. 9(c), the sensor is routed by avoiding the crease line, and the sensor path does not interfere with the propagation of the crease line on the fabric on the elbow and shoulder motion. This enhances the sensing robustness of the bend sensor for joint angle measurement and maintains wear comfort. Although the optimal routing path to determine the point of tension on the sleeve with various postures should be determined using finite element method (FEM) analysis [31], [32], this study focuses on the initial validation of the proposed concept with heuristic placement within the concept of screw routing. The experimental results supporting the effectiveness of screw sensor routing are discussed in the following section.

2) *Sensor Attachment Methods*: To increase the usability of smart work clothes and increase sensing accuracy, the following principles are considered to determine a way to attach the sensor. (1) Easy to attach and detach the sensor with one hand, (2) it must not interfere with the movement of the user, (3) the sensor should not cause unwanted wrinkles on the fabric so as not to impair the sensing accuracy and robustness, (4) there should be no eyesore parts for the aesthetics, (5) it should be able to protect the sensor from the working environment, and (6) it should be possible to attach sensors to ready-made work clothes with minimal modifications.

The method of inserting sensor along the desired sensing path is selected for attaching bend sensor onto the smart work suit considering requirements described above. The desired sensor path satisfying the required principles is enabled by sewing additional guide sleeves to hold the sensors on the inner surface of the work clothes (Fig. 10). The sensor routing sleeves are made of polyester to minimize friction that may occur during the attachment or detachment of the sensors. After inserting the sensor through the eye-button hole, the sensor module pocket fixes the position of the sensor module.

### III. EXPERIMENTAL METHOD

The developed smart work suit is evaluated using commercial inertial measurement units (IMUs; Xsens Awinda) to verify the

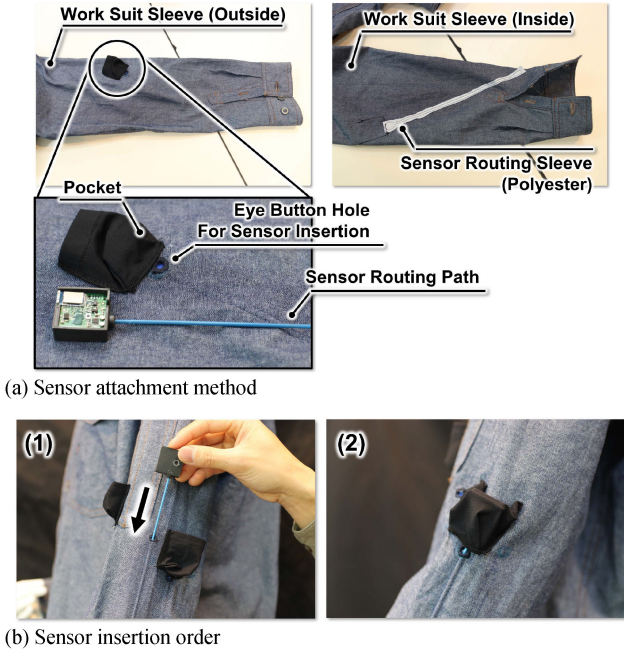


Fig. 10. (a) Sensor attachment method: Sensor guiding sleeve, pockets and eye button holes design. (b) Sequential order to insert the sensor: The sensor can be inserted through the eye button hole to be routed along with the PE guide inside the sleeve.

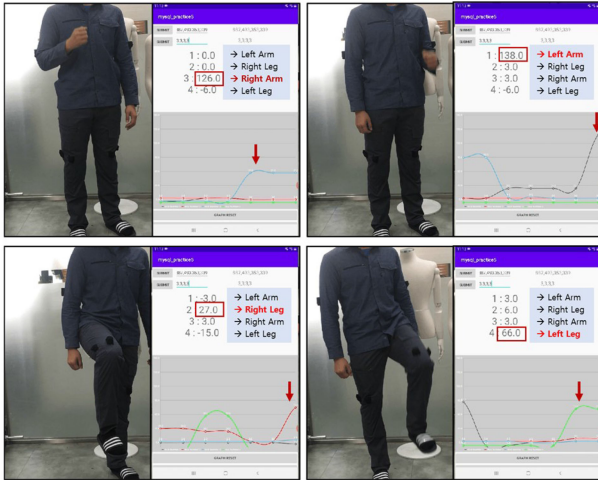


Fig. 11. Measured data from the sensing modules can be wirelessly monitored and saved with multiple devices at the same time using iBeacon protocol which does not require Bluetooth pairing sequence.

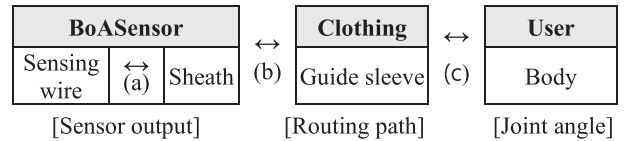
usefulness of the proposed smart work suit system and the sensor routing method. The data of the smart work suit and IMUs are recorded for various postures and motions to investigate the effect of posture-dependent sensor dislocation. The linearity, accuracy, and precision of the sensing system are calculated and compared with those of an IMU.

During the joint angle measurement experiment (Fig. 11) of the upper extremities, we placed the sensor on the work suit using three different paths: elbow dorsal, lateral, and screw-type. The subject wore the smart work suit, took three different shoulder postures, and moved the arm in four different directions (Fig. 12). For the experiment on the lower extremities, sensors

Arm Posture	Movement Direction			
	①F	②P+F	③R+F	④R+P+F
A- Attention				
B- Arm forward				
C- Arm sideward				

Fig. 12. Experimental conditions to test the posture-dependent characteristics of the sensor routing method. The subject took three different arm postures (A: Attention, B: Arm forward, C: Arm sideward) for four different movement direction (F: Flexion, P: Pronation, R: Rotation).

TABLE I  
DIAGRAM OF THE INTERACTION BETWEEN COMPONENTS



were placed on the knee with dorsal and lateral routings to measure the knee joint angles. Each movement was made eight times.

IMUs attached to the subject’s wrist, upper arm, lower arm, torso, pelvis, thigh, and shank provided the orientation of each joint and limb. Orientation data were then integrated using the OpenSim software, on which joint angles were calculated through inverse kinematics using the OpenSense toolkit.

The angle-measuring performance of the smart work suit was evaluated based on three criteria: linearity, precision, accuracy. During human movements, the measurement of the joint angle by the smart work suit largely varies depending on fabric deformation. Thus, it is important to evaluate whether the suit can reliably measure joint angles for various postures.

The accuracy and statistical significance of the smart work suit were measured and calculated using the joint angle measured by the IMUs. In this study, the data from IMUs are presumed ground truth and the accuracy of the IMUs is not taken into account because the measurement of the joint angle is used for estimating macroscopic worker movement patterns during the work environment.

#### IV. RESULTS

First, we analyzed the sensing behavior of the sensing data in terms of linearity. We also examined statistical significance in the angle measurement results between the IMUs and smart work suit to verify the performance and usefulness of the proposed system. Table III, Figs. 15 and 16 present the mean and standard deviation of the elbow and knee angle sensing experiments, respectively to compare the statistical significance of the smart work suit with IMUs. Table IV present the RMSE of the smart work suit according to the sensor routing method in degrees and percentages over the elbow range of motion 150°, respectively.

TABLE II  
NONLINEARITY AND HYSTERESIS ERROR FOR EACH ROUTING METHOD WITH  
THREE POSTURES

Error of RO (%)		A	B	C	Avg.	Max.
Dorsal	Nonlinearity*	34.3	27.3	27.1	29.6 (16.3)	34.3 (20.3)
	Hysteresis†	6.84	14.4	11.2	10.8 (16.4)	14.4 (27.3)
Lateral	Nonlinearity	57.9	40.6	34.1	44.2 (29.7)	57.9 (35.8)
	Hysteresis	30.3	7.64	4.05	14.0 (25.7)	30.3 (35.7)
Screw	Nonlinearity	28.4	14.8	16.6	19.9 (13.4)	28.4 (17.8)
	Hysteresis	17.2	7.60	7.98	10.9 (10.1)	17.2 (14.4)

Units in percentage error of rated output (RO), 150°.

\*Nonlinearity: maximum difference of the sensor output from the ideal linear line.

†Hysteresis: maximum difference of the sensor output of the hysteresis curve.

The values in brackets represent the results of the polynomial fitting.

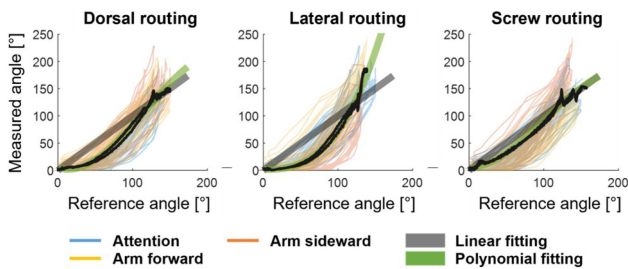


Fig. 13. Measured angle with smart work suit in accordance with the reference joint angle. Each color line - blue, yellow, and orange - illustrates data for three postures with three combined moving directions - attention, arm forward, and arm sideward, respectively. Here, solid black line indicates average value of the measured angle. The grey and green thick lines illustrate linear and polynomial fitting for each routing method.

### A. Sensing Behavior

Fig. 13 shows the measured angle with smart work suit in accordance with the reference joint angle measured with IMUs for dorsal, lateral, and screw routing. Each line color represents a specific posture combined with three movement directions. In contrast to previous studies, the objective of this study is to develop robust sensing methods in a variety of conditions, so each plot includes a total of nine experimental conditions (3 postures x 3 directions), which exhibit some deviation.

There exists hysteresis loop in counter clockwise, which is commonly observed in soft sensors due to elasticity, viscosity, and friction. In the case of the smart work suit system, this is assumed to be a backlash hysteresis that is observed in tendon-sheath mechanisms [33]. The smart work suit is a series of tendon-sheath mechanisms, as shown in Table I, and has nonlinearity similar to tendon-drive systems. Fig. 14 shows the cross-sectional view of the dead-zone model of the sensor. Since the BoASensor estimates bending angles by measuring the displacement change of the sensing wire inside the sheath when the sensor bends [22], there is an inevitable dead-zone at the early response due to the clearance between the inner diameter of the sheath ( $d_1$ ) and the diameter of the sensing wire ( $d_2$ ). A geometrical calculation can be made to determine the sensing dead-zone ( $\theta_{dead}$ ), up to which the displacement of the sensing wire does not change at the initial bend of the BoASensor. Here,  $\kappa$  illustrate the bend curvature of the sensor and  $\Delta d = d_1 - d_2$

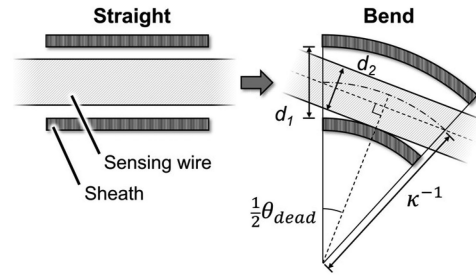


Fig. 14. Cross-sectional view of the dead-zone model of the BoASensor.

is the clearance.

$$\theta_{dead} = 2 \cdot \cos^{-1} \left( 1 - \frac{1}{2} \kappa \cdot \Delta d \right) \quad (1)$$

The same principle applies to the relationship between BoASensor and guide sleeve on clothing—Table I(b)—and to the relationship between body and clothing's sleeve—Table I(c). These factors cumulatively increase the nonlinear region in the relationship between the joint angle of the user and the sensor's output. Since the curvature of the sensor when measuring elbow joint ranges from 0.01 to 0.015 mm<sup>-1</sup>, and the clearance of the sensor is 0.3 mm (0.5mm of sheath inner diameter, 0.2mm of sensing wire diameter), the theoretical dead-zone for BoASensor is 6~8°, and the smart work suit should have larger dead-zone as can be seen in Fig. 13. There is a dead-zone of 10 to 20° for dorsal and lateral routing. Using dorsal and lateral routing, BoASensor measures the joint angle from the zero bending of the sensor, so the dead-zone is unavoidable. Screw routing method helps to alleviate these nonlinearities of Table I (a)–(c) by pre-bending the sensor along the routing path. The routing path of screw routing is pre-bent at the initial state removing the effect of clearance in the relation Table I (a) and (b).

Additionally, the sensitivity of the sensor, which is a slope of the output curve (deg/deg), increases with reference angle and converges at a certain point. The elasticity of the mechanical parts (the sensing wire, sheath, and tensioning spring in the case of BoASensor) acts as a damping between the dead-zone and the linear zone.

Table II presents the nonlinearity error and the hysteresis error for each routing method with three postures. Each posture includes three different moving directions. To simplify many cases, errors are calculated based on the average measured angle, with different moving directions for each routing method and posture. It is observed that the lateral routing has the highest nonlinearity error, 44.2% of RO and the screw routing has the lowest, 19.9% of RO in average. The lateral routing also showed the largest hysteresis error, 14.0% of RO while the screw routing showed 10.9% of RO in average. Additionally, the lateral routing had the largest maximum nonlinearity error and hysteresis error, while the screw routing had the lowest maximum nonlinearity error. Overall, the screw routing showed the best linear behavior. In practice, the nonlinear behavior of the system can be further reduced by fitting polynomials, which show 13.4% and 10.1% nonlinearity and hysteresis error, respectively.

### B. Precision

Precision was chosen as a performance factor for the proposed system because the main contribution of screw sensor routing

TABLE III  
EXPERIMENTAL RESULTS OF SENSING PRECISION FOR ELBOW

Motion	Sensor	Dorsal routing			Lateral routing			Screw routing		
		A	B	C	A	B	C	A	B	C
①	BoA	24.01	13.14	14.51	17.18	28.87	17.12	10.23	14.52	19.20
	IMU	12.12	10.15	6.26	8.17	11.35	8.82	9.51	11.50	12.42
②	BoA	18.68	13.19	13.61	16.00	17.10	15.84	12.49	9.13	18.29
	IMU	7.83	9.98	9.74	8.34	12.65	10.09	13.60	12.49	16.30
③	BoA	10.44	19.23	18.42	23.03	18.07	15.03	10.69	18.15	12.55
	IMU	10.58	6.36	9.65	11.34	11.36	11.25	12.02	14.46	18.49
④	BoA	15.90	19.02	17.64	21.24	23.26	17.34	14.12	12.91	19.90
	IMU	12.00	10.02	12.04	11.38	15.95	17.65	17.94	14.26	26.09
<i>U-test p-value</i>		0.200	0.029	0.029	0.029	0.029	0.343	0.886	0.686	0.886

Units in degree

A, B, and C indicate the posture of the Arm and ①–④ indicate direction of motion for each postures.

TABLE IV  
EXPERIMENTAL RESULTS OF SENSING ACCURACY FOR ELBOW

Motion	Dorsal routing			Lateral routing			Screw routing		
	A	B	C	A	B	C	A	B	C
①	2.92	8.18	10.74	10.14	22.19	16.65	7.39	9.42	13.83
②	7.95	5.76	3.90	3.46	16.57	17.25	8.19	4.89	10.67
③	3.11	19.82	3.90	10.85	2.73	7.57	6.20	3.67	3.38
④	3.77	14.27	5.60	22.93	14.55	4.55	7.78	7.44	10.15
<i>Sensing Error</i>	$\mu: 7.49, \sigma: 4.96$			$\mu: 12.45, \sigma: 6.69$			$\mu: 7.75, \sigma: 2.90$		

Units in percentage of elbow range of motion ( $150^\circ$ ),  $\mu$ : mean,  $\sigma$ : standard deviation

A, B, and C indicate the posture of the Arm and ①–④ indicate direction of motion for each postures.

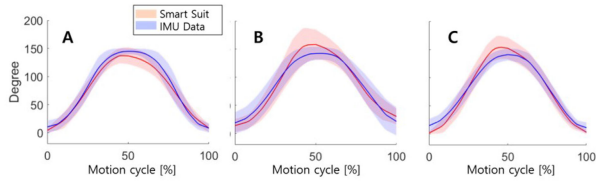


Fig. 15. Elbow angle sensing results tracked by the smart work suit (in red) and IMU (in blue) for the arm posture A, B, and C with various movement directions in Fig. 12 for motion cycle phase. Solid lines indicate mean value at the corresponding motion cycle, while the shaded area indicates standard deviation.

is reducing the pose-dependent error of the smart work suit. Table III presents the standard deviation of the joint angle measured in the arm movement experiments, depending on the sensor attachment locations, shoulder postures, and movement directions. It should be noted that the participants' natural variability of movement was a confounding factor. We tested for statistical significance between the smart work suite and IMUs using the Mann–Whitney U-test. The results of the U-test indicate that the screw routing method had a closer level of precision as the IMU data within the significance level of 5%; p-values were 0.886, 0.686, and 0.886 for postures A, B, and C, respectively, while the dorsal routing and lateral routing failed to satisfy the criteria; p-values of B and C postures for dorsal, and A and B postures for lateral routing were 0.029. This can be explained by the fact that the screw routing method can minimize the effects of pose-dependent errors compared with the dorsal and lateral direction routing methods.

The dynamic behavior of the screw routing method can be visualized for three arm postures, A, B, and C, during the motion cycle, as illustrated in Fig. 15. The shaded lines are centered

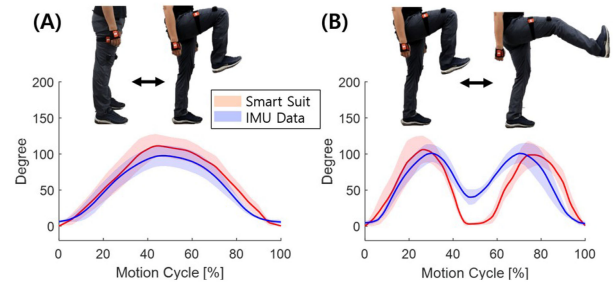


Fig. 16. Knee angle sensing results in motion cycle phase as tracked by the developed suit (in red) and IMU (in blue) with the leg posture A and B. Solid line indicates mean value at the corresponding motion cycle, while the shaded area indicates standard deviation.

at the mean value, which is drawn as a solid line, while the width indicates the standard deviation from the mean. Fig. 16 illustrates the angle-sensing results of the sensor attached with the dorsal routing for the knee joint. It has an average standard deviation of  $13.47^\circ$ , confirming that the reliability is sufficient compared with the IMUs, which have a standard deviation of  $10.94^\circ$ . The sensor attached with the lateral routing could not properly measure the joint angle, owing to the excessive fabric deformation.

### C. Accuracy

Table IV present the experimental results for the accuracy assessment of the elbow joint of the smart work suits with various upper-body postures and sensor routing methods. It can be observed that the screw routing method had the smallest standard deviation with 2.90 and low sensing error with 7.75% of RO for various upper body postures within the elbow range of

motion (0–150°). Although the dorsal and lateral routing method have the advantage that it can follow the elbow flexion owing to its straight structure, it is vulnerable to the rotation of the sleeves during various movements as depicted in Fig. 9(a). Thus, accuracy of the dorsal direction routing method varies significantly, while screw routing can maintain a reliable performance. For the knee joint, the sensor attached in the knee direction had RMSE of 10.33° on the knee raising movement, which corresponds to an error of 7.65% compared with the knee range of motion (0–135°).

## V. CONCLUSION

We proposed a smart work suit that can measure the movements of the wearer using a modular bend sensor. It was verified that the proposed sensor routing mechanism is advantageous in increasing the sensing reliability with the work jacket and trousers in a loose fit. The proposed system is affordable, with which the sensing module can be manufactured at low prices (under 30 USD) and with only a small modification—adding a PE sleeve for sensor routing—a ready-made work suit turns into a motion-sensing smart work suit. Despite the large measuring nonlinearities of the smart work suit system due to the loose fit of the clothing and the 1-dof sensing data, there is a compromise between the usability and the performance. The linearity of the system can be improved by minimizing the mechanical clearance and friction along the system in Table I. Additionally, nonlinear calibration can be adopted using a hysteresis model, such as the Bouc-Wen model [33]. A neural-net based calibration is another candidate [16], which has been used with soft sensors in recent years. In order to distinguish the angle of the target joint from various postures and combined motion, multi-degrees of freedom sensors like IMUs should be used. The proposed smart work suit can be utilized in various places, requiring a simple interface, including manufacturing, warehouse, and even at home or in the office. The collected motion data can be utilized in the future to monitor the manufacturing process variables in the factory-worker network or manage the work intensity and health of the employee.

## REFERENCES

- [1] C. Cimini, F. Pirola, R. Pinto, and S. Cavalieri, “A human-in-the-loop manufacturing control architecture for the next generation of production systems,” *J. Manuf. Syst.*, vol. 54, pp. 258–271, 2020.
- [2] C. J. Turner, R. Ma, J. Chen, and J. Oyekan, “Human in the loop: Industry 4.0 technologies and scenarios for worker mediation of automated manufacturing,” *IEEE Access*, vol. 9, pp. 103950–103966, 2021.
- [3] R. J. Simonson, J. R. Keebler, E. L. Blickensderfer, and R. Besuijen, “Impact of alarm management and automation on abnormal operations: A human-in-the-loop simulation study,” *Appl. Ergonom.*, vol. 100, 2022, Art. no. 103670.
- [4] Z. Arman, M. Nikooy, P. A. Tsioras, M. Heidari, and B. Majnounian, “Physiological workload evaluation by means of heart rate monitoring during motor-manual clearcutting operations,” *Int. J. For. Eng.*, vol. 32, no. 2, pp. 91–102, May 2021.
- [5] P. Bhavsar, B. Srinivasan, and R. Srinivasan, “Pupillometry based real-time monitoring of operator’s cognitive workload to prevent human error during abnormal situations,” *Ind. Eng. Chem. Res.*, vol. 55, no. 12, pp. 3372–3382, Mar. 2016.
- [6] “Vicon,” *Vicon*. Accessed: Jul. 2022. [Online]. Available: <https://www.vicon.com/>
- [7] Xsens, “Xsens 3D motion tracking.” Accessed: Jul. 2022. [Online]. Available: <https://www.xsens.com>
- [8] W. Tao, Z.-H. Lai, M. C. Leu, and Z. Yin, “Worker activity recognition in smart manufacturing using IMU and sEMG signals with convolutional neural networks,” *Procedia Manuf.*, vol. 26, pp. 1159–1166, 2018.
- [9] M. Donno, E. Palange, F. Di Nicola, G. Bucci, and F. Ciancetta, “A new flexible optical fiber goniometer for dynamic angular measurements: Application to human joint movement monitoring,” *IEEE Trans. Instrum. Meas.*, vol. 57, no. 8, pp. 1614–1620, Aug. 2008.
- [10] O. Patsadu, C. Nukoolkit, and B. Watanapa, “Human gesture recognition using Kinect camera,” in *Proc. IEEE 9th Int. Conf. Comput. Sci. Softw. Eng. (JCSSE)*, May 2012, pp. 28–32.
- [11] A. P. L. Bó, M. Hayashibe, and P. Poignet, “Joint angle estimation in rehabilitation with inertial sensors and its integration with Kinect,” in *Proc. IEEE Annu. Int. Conf. Eng. Med. Biol. Soc.*, Aug. 2011, pp. 3479–3483.
- [12] T. Schlömer, B. Poppinga, N. Henze, and S. Boll, “Gesture recognition with a Wii controller,” in *Proc. 2nd Int. Conf. Tangible Embedded Interaction*, New York, NY, USA, Feb. 2008, pp. 11–14.
- [13] S. J. Ray and J. Teizer, “Real-time construction worker posture analysis for ergonomics training,” *Adv. Eng. Inform.*, vol. 26, no. 2, pp. 439–455, Apr. 2012.
- [14] W. Park, K. Ro, S. Kim, and J. Bae, “A soft sensor-based three-dimensional (3-D) finger motion measurement system,” *Sensors*, vol. 17, no. 2, Feb. 2017, Art. no. 2.
- [15] F. L. Hammond, Y. Mengüç, and R. J. Wood, “Toward a modular soft sensor-embedded glove for human hand motion and tactile pressure measurement,” in *Proc. IEEE/RSJ Int. Conf. Intell. Robots Syst.*, Sep. 2014, pp. 4000–4007.
- [16] D. Kim, J. Kwon, S. Han, Y.-L. Park, and S. Jo, “Deep full-body motion network for a soft wearable motion sensing suit,” *IEEE/ASME Trans. Mechatron.*, vol. 24, no. 1, pp. 56–66, Feb. 2019.
- [17] M. Totaro et al., “Soft smart garments for lower limb joint position analysis,” *Sensors*, vol. 17, no. 10, Oct. 2017, Art. no. 10.
- [18] H. Chander et al., “Wearable stretch sensors for human movement monitoring and fall detection in ergonomics,” *Int. J. Environ. Res. Public Health*, vol. 17, no. 10, May 2020, Art. no. 3554.
- [19] E. S. Varaki, P. P. Breen, and G. D. Gargiulo, “Quantification of a low-cost stretchable conductive sensor using an expansion/contraction simulator machine: A step towards validation of a noninvasive cardiac and respiration monitoring prototype,” *Machines*, vol. 5, no. 4, Dec. 2017, Art. no. 4.
- [20] M. C. Yuen, H. Tonoyan, E. L. White, M. Telleria, and R. K. Kramer, “Fabric sensory sleeves for soft robot state estimation,” in *Proc. IEEE Int. Conf. Robot. Automat.*, May 2017, pp. 5511–5518.
- [21] W. S. Lee et al., “Designing metallic and insulating nanocrystal heterostructures to fabricate highly sensitive and solution processed strain gauges for wearable sensors,” *Small*, vol. 13, no. 47, 2017, Art. no. 1702534.
- [22] U. Jeong and K.-J. Cho, “A novel low-cost, large curvature bend sensor based on a bowden-cable,” *Sensors*, vol. 16, no. 7, Jul. 2016, Art. no. 7.
- [23] “Biometrics Ltd.” Accessed: Jul. 2022. [Online]. Available: <https://www.biometricsltd.com/goniometer>
- [24] P. Rowe, C. Myles, S. Hillmann, and M. Hazlewood, “Validation of flexible electrogoniometry as a measure of joint kinematics,” *Physiotherapy*, vol. 87, no. 9, pp. 479–488, Sep. 2001.
- [25] S. Ashdown, *Sizing in Clothing*. Amsterdam, The Netherlands: Elsevier, 2007.
- [26] K. Wolff, P. Herholz, V. Ziegler, F. Link, N. Brügel, and O. Sorkine-Hornung, “3D Custom fit garment design with body movement,” Feb. 2021. [Online]. Available: <http://arxiv.org/abs/2102.05462>
- [27] F. Uddin, *Textile Manufacturing Processes*. IntechOpen, 2019. [Online]. Available: <https://www.intechopen.com/books/8892>
- [28] P. Guan, L. Reiss, D. A. Hirshberg, A. Weiss, and M. J. Black, “Drape: Dressing any person,” *ACM Trans. Graph. TOG*, vol. 31, no. 4, pp. 1–10, 2012.
- [29] V. Masteikaitė, V. Sacevičienė, and V. Čironienė, “Compressed loop method for the bending behaviour of coated and laminated fabrics analysis,” *J. Ind. Textiles*, vol. 43, no. 3, pp. 350–365, Jan. 2014.
- [30] S. Bragança, P. Azees, M. Carvalho, and S. Ashdown, “Implications of dynamic working postures in garments’ comfort,” in *Proc. 6th Int. Ergonom. Conf.*, 2016, pp. 31–38.
- [31] X. Zhang, K. W. Yeung, and Y. Li, “Numerical simulation of 3D dynamic garment pressure,” *Textile Res. J.*, vol. 72, no. 3, pp. 245–252, Mar. 2002.
- [32] T. L. Kunii and H. Gotoda, “Modeling and animation of garment wrinkle formation processes,” in *Computer Animation '90*. Tokyo, Japan: University of Tokyo, 1990, pp. 131–147.
- [33] T. N. Do, T. Tjahjowidodo, M. W. S. Lau, T. Yamamoto, and S. J. Phee, “Hysteresis modeling and position control of tendon-sheath mechanism in flexible endoscopic systems,” *Mechatron.*, vol. 24, no. 1, pp. 12–22, Feb. 2014.